



CRYSTALLOGRAPHIC AND THEORETICAL STUDIES ON A COUPLED CHAIN OF AF BINUCLEAR CU(II)-FLUORASPIRINATE COMPLEXES

C. A. Lamas^(a), O. E. Piro^{(a)*}, E. E. Castellano^(b), E. M. Rustoy^(c) and O. V. Quinzani^(c)

^(a)Depto. de Física, Ftad de C. Exactas, UNLP and IFLP (CONICET), C.C. 67, 1900, La Plata, Argentina,

^(b)Inst. de Física de São Carlos, Universidade de São Paulo, Cx.P. 369 São Carlos, SP, 13566-590, Brazil.

^(c)Depto. de Química, Universidad Nacional del Sur, Avda. Alem 1253, B8000CPB, Bahía Blanca, Argentina

*e-mail: piro@fisica.unlp.edu.ar

ABSTRACT. We present here the low temperature (116K) crystal and molecular structure of poly- $[\mu$ -pyrazine{tetrakis-fluoraspirinate-dicopper(II)}]diacetonitrile, for short $[\text{Cu}(\text{Fasp})_4\text{Cu}(\text{pyz})]_n$, a 5-halogenated derivative of pharmacologically relevant copper aspirinates. We also discuss the theoretically expected magnetic and thermodynamic behavior of this interesting system for molecular magnetism.

Key words: Crystallography, Molecular Magnetism, Coupled AF Binuclear Complexes

1. Introduction

Dicopper(II) carboxylate complexes exhibiting a lantern-like structure have been the object of intense research.^{1,2} Earlier studies on the structural and magnetic properties of the prototypic copper acetate were considered key for the understanding of super-exchange paths in dinuclear compounds and in the development of appropriate models to describe the magnetic coupling between metal centers.^{3,4} Numerous studies have been carried out on the biological activity of copper carboxylates. In particular, copper aspirinates have been found to act as anti-inflammatory, analgesic, anti-carcinogenic, anticonvulsant, antithrombotic, catecholase mimetic and potential neuron-protective agents.^{5,6} These pharmacological studies often contain copper-aspirinate systems either involving simple mononuclear complexes or *paddle-wheel* binuclear tetrakis-aspirinate complexes. In contrast with the large number of experimental and theoretical studies about aspirin,^{6,7} less is known about its 5-halogenated derivatives. We report here the X-ray crystal and molecular structure of polymeric $[\text{Cu}(\text{Fasp})_4\text{Cu}(\text{pyz})]_n$ and present numerical results on the magnetic and thermodynamic behavior of the coupled chain of anti-ferromagnetic (AF) binuclear copper(II) complexes as a function of the inter-dimer super-exchange coupling constant.

2. X-ray diffraction data and structure solution and refinement

The measurements were performed at low temperature on an Enraf-Nonius Kappa-CCD diffractometer with graphite-monochromated $\text{MoK}\alpha$ ($\lambda=0.71073$ Å) radiation. Diffraction data were collected (φ and ω scans with κ -offsets) with COLLECT.⁸ Integration and scaling of the reflections was performed with HKL DENZO-SCALEPACK⁹ suite of programs. The unit cell parameters were obtained by least-squares refinement based on the angular settings for all collected reflections using

HKL SCALEPACK.⁹ The data were corrected empirically for absorption with the multi-scan procedure.¹⁰ The structure was solved by direct methods with SHELXS-97¹¹ and the molecular model refined by full-matrix least-squares procedure with SHELXL-97.¹² The hydrogen atoms were positioned stereo-chemically and refined with the riding model. The methyl hydrogen atoms locations were optimized during the refinement by treating them as rigid bodies which were allowed to rotate around the corresponding C-CH₃ bond. Crystal data and structure refinement results are summarized in Table 1.

Table 1. Crystal data and structure refinement results for $[\text{Cu}_2(\text{Fasp})_4(\text{pyz})]_n$.

Empirical formula	$\text{C}_{44}\text{H}_{34}\text{Cu}_2\text{F}_4\text{N}_4\text{O}_{16}$
Formula weight	1077.83
Temperature (K)	116(2)
Wavelength (Å)	0.71073
Crystal system	Triclinic
Space group	P-1 (#2)
Unit cell dimensions	
a(Å)	9.8900(2)
b(Å)	11.0850(3)
c(Å)	11.7900(3)
α (°)	78.818(1)
β (°)	65.294(1)
γ (°)	73.048(1)
Volume(Å ³)	1119.34(5)
Z, calculated density (Mg/m ³)	1, 599
Absorption coefficient (mm ⁻¹)	1.045
F(000)	414
Crystal size (mm)	0.24 x 0.16 x 0.10
Crystal color/shape	Blue / prismatic
ϑ range for data collection (°)	1.93 to 25.99
Index ranges	-12 \leq h \leq 12, -13 \leq k \leq 13, -14 \leq l \leq 14
Reflections collected / unique	15470/4409 [R(int)=0.061]
Completeness (%)	99.9 (to $\vartheta=25.99^\circ$)
Observed reflections [I>2 σ (I)]	3987

Max. and min. transmission	0.9027 and 0.7876
Refinement method	Full-matrix least-squares on F^2
Weights, w	$[\sigma^2(F_o^2) + (0.06P)^2 + 0.99P]^{-1}$ $P = [\text{Max}(F_o^2, 0) + 2F_c^2]/3$
Data / restraints / parameters	4409 / 0 / 314
Goodness-of-fit on F^2	1.039
Final R indices* $[I > 2\sigma(I)]$	$R_1 = 0.0375$, $wR_2 = 0.1031$
R indices (all data)	$R_1 = 0.0433$, $wR_2 = 0.1071$
Largest peak and hole	0.699 and -0.908 $e \cdot \text{\AA}^{-3}$

$$*R_1 = \frac{\sum ||F_o| - |F_c||}{\sum |F_o|}, wR_2 = \frac{[\sum w(|F_o|^2 - |F_c|^2)^2 / \sum w(|F_o|^2)]^{1/2}}$$

3. Structural results

Figure 1 shows an ORTEP¹³ drawing of the molecule. Intra-molecular bond distances and angles around copper(II) in $[\text{Cu}(\text{Fasp})_4\text{Cu}(\text{pyz})]_n$ are in Table 2.

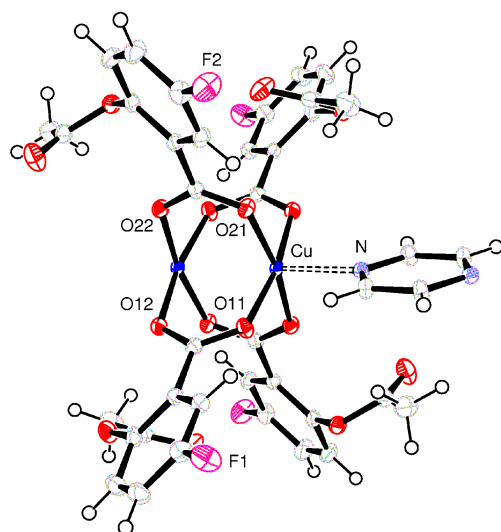


Figure 1. Molecular plot showing one monomer of the $[\text{Cu}(\text{Fasp})_4\text{Cu}(\text{pyz})]_n$ polymer. The $\text{Cu}(\text{Fasp})_4\text{Cu}$ dimer and the axially bonded-to-copper pyrazine molecule are sited on crystallographic inversion centers. For clarity, only the oxygen atoms of the bridging carboxylic groups and the pyrazine nitrogen along with the aspirinate F-atoms are labeled. Carbon atoms are indicated by light crossed disks. The displacement ellipsoids of the non-H atoms are drawn at the 50% probability level.

Table 2. Intra-molecular bond distances (\AA) and angles ($^\circ$) around Cu(II) in $[\text{Cu}_2(\text{Fasp})_4(\text{pyz})]_n$.*

Bond distances	
Cu-O(22')	1.964(2)
Cu-O(21)	1.965(2)
Cu-O(11)	1.967(2)
Cu-O(12')	1.974(2)
Cu-N	2.233(2)

Cu-Cu' 2.6417(5)

Bond angles

O(22')-Cu-O(21)	168.59(7)
O(22')-Cu-O(11)	89.09(7)
O(21)-Cu-O(11)	89.71(7)
O(22')-Cu-O(12')	89.60(7)
O(21)-Cu-O(12')	89.34(7)
O(11)-Cu-O(12')	168.61(7)
O(22')-Cu-N	99.23(7)
O(21)-Cu-N	92.15(7)
O(11)-Cu-N	91.46(7)
O(12')-Cu-N	99.92(7)
O(22')-Cu-Cu'	82.96(5)
O(21)-Cu-Cu'	85.64(5)
O(11)-Cu-Cu'	85.18(5)
O(12')-Cu-Cu'	83.43(5)
N-Cu-Cu'	175.98(5)

re related to the corresponding unprimed inversion symmetry operation: $-x+1, -y, -z+1$

$[d(\text{Cu}\dots\text{Cu}) = 2.6417(5) \text{ \AA}]$ dimeric group tallocraphic inversion center and shows a formation where the Cu(II) ions are bridged by four Fasp groups acting as bidentate near carboxylic oxygen atoms [Cu-O bond 1.964(2) to 1.974(2) \AA]. Neighboring units in the lattice are axially linked by $\text{C}_4\text{H}_4\text{N}$ groups (also on an inversion center) [Cu-N = 2.233(2) \AA] giving rise to $1\dots\text{N}(\text{C}_4\text{H}_4)\text{N}\dots\text{Cu}(\text{Fasp})_4\text{Cu}\dots$ polymeric chains along the crystal a -axis (see in Fig. 2). This structure agrees well with $[\text{H}_3\text{CO}_2]_4(\text{pyz})_n$ and $[\text{Cu}_2(\text{CH}_3\text{CO}_2)_4(\text{pyz})]_n$; ^{15, 16}

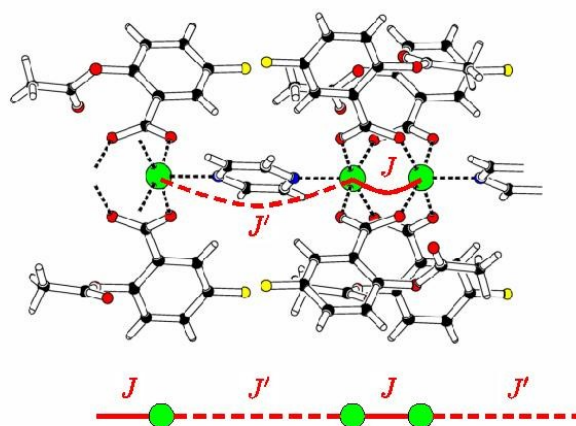


Figure 2. Molecular diagram showing part of the $[\text{Cu}(\text{Fasp})_4\text{Cu}(\text{pyz})]_n$ polymer and the labeling of the super-exchange coupling constants referred to in the theoretical calculations. Large green disks indicate Cu(II) ions, while the red, blue, yellow and black smaller disks denote oxygen, nitrogen, fluorine and carbon atoms, respectively.

4. Theoretical results

4.1. Spin Hamiltonian of isolated AF dimer

As for other lantern-structured copper carboxylates, the (pyz)₂Cu(Fasp)₂Cu(py₂) dimer constitutes a system with two antiferromagnetically (AF) coupled $S = 1/2$ centers. The intra-dimer magnetic behavior of the copper unpaired electrons ($S_1 = S_2 = 1/2$) in an external magnetic field \mathbf{H} can be described by the following Hamiltonian:³

$$H = (V_1 + V_2) - J\mathbf{S}_1 \cdot \mathbf{S}_2 + \gamma(\mathbf{L}_1 \cdot \mathbf{S}_1 + \mathbf{L}_2 \cdot \mathbf{S}_2) + \beta \mathbf{H}(\mathbf{L}_1 + 2\mathbf{S}_1 + \mathbf{L}_2 + 2\mathbf{S}_2), \quad (1)$$

where the first term describes ligand field effects, the second is the exchange coupling between the electrons, and the third and fourth contributions are the spin-orbit and Zeeman interactions. The crystal field effects lead to a mainly metal $d(x^2-y^2)$ ground state orbital with its lobes along the Cu-O bonds (nearly along the x and y axes), energetically well separated from the electronic excited states. The exchange interaction produces the largest (first-order) perturbation to the spin fourfold-degenerated ground state by splitting it into a diamagnetic singlet ground state (total spin $S = 0$) and a paramagnetic triplet ($S = 1$) excited level, energy-separated in $|J|$. Perturbation theory up to second-order, including exchange, spin-orbit and Zeeman interactions, shows that the triplet state can be described by the effective spin ($S = 1$) Hamiltonian

$$H_{eff} = \mathbf{S} \cdot \mathbf{D} \cdot \mathbf{S} + \beta \mathbf{S} \cdot \mathbf{g} \cdot \mathbf{H}, \quad (2)$$

where \mathbf{D} and \mathbf{g} are the fine and gyromagnetic tensors, respectively. The fine interaction splits the triplet state in the absence of an external magnetic field into a singlet ($S_z = 0$) and a doublet ($S_z = \pm 1$). It arises from the combined effect of ligand field, exchange and spin-orbit interactions and vanishes for uncoupled ($J = 0$) electrons. The symmetric \mathbf{D} and \mathbf{g} tensors share the same principal (x, y, z) axes, where the spin Hamiltonian adopts the form

$$H_{eff} = DS_z^2 + E(S_x^2 + S_y^2) + \beta(g_x H_x S_x + g_y H_y S_y + g_z H_z S_z). \quad (3)$$

Single-crystal EPR measurements in the closely related system of $\text{Cu}_2(\text{CH}_3\text{CO}_2)_4(\text{H}_2\text{O})_2$ shows that the dimer exhibits approximate axial symmetry and therefore $E \approx 0$, $g_x \approx g_y \approx g_\perp$ and $g_z = g_\parallel$.³ Assuming the same holds for our system, (3) further simplifies to

$$H_{eff} = DS_z^2 + \beta [g_\perp (H_x S_x + g_y S_y) + g_\parallel H_z S_z]. \quad (4)$$

The fine and Zeeman interactions (a fraction of 1 cm^{-1}) are much smaller than the exchange interaction (in the present case, a few hundredths of a cm^{-1}). This interaction, in turn, is

much less than the energy separation between electronic ground and excited states. This warrants the description of the powder molar magnetic susceptibility of isolated AF dimers by the Van Vleck expression, which to second-order approximation leads to the Bleaney-Bowers equation³

$$\chi(T) = \frac{2N_A g^2 \beta^2}{kT [3 + \exp(-J/kT)]}, \quad (5)$$

where N_A is the Avogadro's number, g the average gyromagnetic factor and β the Bohr magneton.

4.2. Coupled chain of AF dimers

Previous EPR spectroscopic work on the related $[\text{Cu}_2(\text{CH}_3\text{CO}_2)_4(\text{pyz})]_n$ polymer concluded that the exchange interaction between dimers, $|J'|$, is much smaller than the intra-dimer $|J|$ value (usually of the order of 400K) and therefore more difficult to measure and interpret since very low temperatures are required and other effects of the same order of magnitude need to be taken into consideration.¹⁵

We present here a preliminary theoretical effort to predict the magnetic and thermodynamic behavior of a coupled chain of AF units as a function of the inter-dimer coupling constant J' (see Fig. 2). To this purpose, we calculated the low-lying energy levels and eigenvector of the system defined by the spin Hamiltonian:

$$H_{eff} = -J \sum_{i=1}^N [\mathbf{S}_{2i} \cdot \mathbf{S}_{2i-1} + \alpha \mathbf{S}_{2i} \cdot \mathbf{S}_{2i+1}], \quad (6)$$

where N is the number of AF dimers and $\alpha = J'/J$, employing the Lanczos' algorithm. From this spectrum we obtained the magnetic susceptibility and specific heat of the chain as a function of temperature. The numerical results for the susceptibility $\chi(T)$ are shown in Fig. 3.

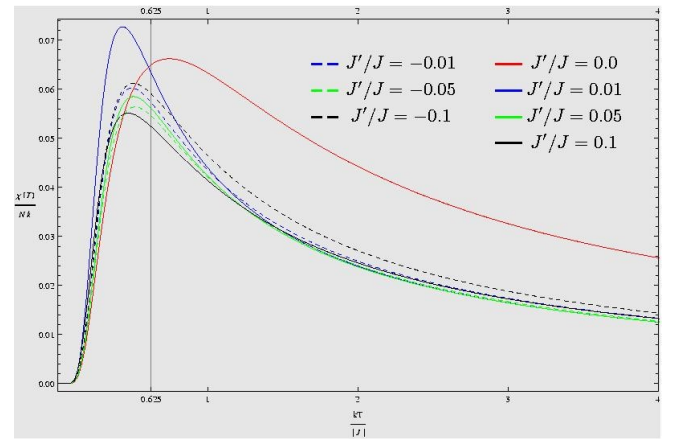


Figure 3. Magnetic susceptibility $\chi(T)$ for a chain of $N=20$ coupled AF dimers. The red curve ($J'/J = 0$) corresponds to an isolated AF with $J = -400\text{K}$. The vertical line at $kT/|J| = 0.625$ indicates the maximum of $\chi(T)$ calculated with the Bleaney-Bowers' equation (5).

From Fig. 3 we can appreciate that the inter-dimer coupling would produce a shift in the susceptibility maximum toward

lower temperatures, which should be experimentally detectable even for relatively weak intra-dimer super-exchange interactions.

Acknowledgments. This work was supported by CONICET of Argentina and FAPESP of Brazil.

References

1. R.C. Mehrotra and R. Bohra, *Metal Carboxylates*. London: Academic Press (1983).
2. M. Kato and Y. Muto, *Coord. Chem. Rev.* 92 (1988), 45-83.
3. B. Bleaney and K.D. Bowers, *Proc. R. Soc. London Sect. A*, 214 (1952), 451-465.
4. O. Kahn, *Molecular Magnetism*, Weinheim: VCH Publishers, Inc. (1993), pp. 103-120.
5. J.E. Weder et al., *Coord. Chem. Rev.* 232 (2002), 95.
6. J.R. Vane and R.M. Bottling (Eds.), *Aspirin and Other Salicylates*, Chapman and Hall, London (1992).
7. X. Wang, *Medical Hypotheses* 50 (1998) 239.
- 8.** *Enraf-Nonius (1997-2000). COLLECT*. Nonius BV, Delft, The Netherlands.
- 9.** Z. Otwinowski and W. Minor, In *Methods in Enzymology* 276, edited by C.W. Carter Jr and R.M. Sweet, New York: Academic Press (1997) pp. 307-326.
10. R.H. Blessing, *Acta Cryst.* A51, 33-38, 1995.
- G.M. Sheldrick, *SHELXS-97. Program for Crystal Structure Resolution*. Univ. of Göttingen: Göttingen, Germany (1997).
12. G.M. Sheldrick, *SHELXL-97. Program for Crystal Structures Analysis*. Univ. of Göttingen: Göttingen, Germany (1997).
13. C.K. Johnson, *ORTEP. Report ORNL-5138*, Oak Ridge, TN (1976).
14. A.L. Spek, *Acta Cryst.*, Sect A 46 (1990), C34.
15. B. Morosin and R.H. Hughes, *Acta Cryst.* B31 (1975), 762-770.
16. S. Takamizawa, E. Nakata and T. Saito, *Inorg. Chem. Comm.* 7 (2004), 1-3